Acta Pharmacologica Sinica (2011) 32: 1505–1512
 1671-4083/11 $32.00
www.nature.com/aps

Original Article

Ganoderma lucidum polysaccharides reduce methotrexate-induced small intestinal damage in mice via induction of epithelial cell proliferation and migration

Li-hua CHEN[1, 2], Zhi-bin LIN[1], Wei-dong LI[1, *]

[1]*Department of Pharmacology, School of Basic Medical Sciences, Peking University Health Science Center, Beijing 100083, China;*
[2]*Department of Clinical Laboratory Science, Changsha Medical University, Changsha 410219, China*

Aim: To study the effects of *Ganoderma lucidum* polysaccharides (G*l*-PS) on methotrexate (MTX)-induced small intestinal damage in mice and the underlying mechanisms.
Methods: BALB/c mice were used for *in vivo* study. The mice were administered with G*l*-PS (50, 100, or 200 mg/kg, ig) for 10 d, and injected with MTX (50 mg/kg, ip) on d 7 and 8 to induce intestinal damage, and then sacrificed on d 11 for morphological study and tissue malondialdehyde (MDA) and superoxide dismutase (SOD) measurements. Before sacrificing, blood samples were collected to analyze immunoglobulin A (IgA). Rat intestinal IEC-6 cells were used for *in vitro* study. Cell proliferation and migration were assessed using MTT method and an *in vitro* wounding model, respectively. Transforming growth factor β (TGFβ) protein expression was determined using ELISA assay. Ornithine decarboxylase (ODC) and c-Myc mRNA expression profiles were determined using RT-PCR.
Results: MTX treatment caused severe mucosal damage, significantly increased small intestine MDA levels, and decreased SOD and serum IgA levels in BALB/c mice. G*l*-PS (100 and 200 mg/kg) markedly reversed the MTX effects. In IEC-6 cells, G*l*-PS (0.1, 1, and 10 μg/mL) significantly stimulated the cell proliferation. Furthermore, G*l*-PS (10 μg/mL) significantly stimulated the cell migration. In addition, G*l*-PS (10 and 20 μg/mL) significantly increased the expression of ODC and c-Myc mRNAs. However, G*l*-PS (up to 20 μg/mL) had no effect on the expression of TGFβ protein.
Conclusion: The results suggest that G*l*-PS protects small intestine against MTX-induced injury via induction of epithelial cell proliferation and migration.

Keywords: *Ganoderma lucidum* polysaccharides; chemotherapy; methotrexate; small intestine injury; IEC-6 cell line

Acta Pharmacologica Sinica (2011) 32: 1505–1512; doi: 10.1038/aps.2011.126; published online 24 Oct 2011

Introduction

The intestinal mucosa barrier (IMB), which is the first line of defense against a hostile environment, is composed of a single layer of columnar epithelium with inter-epithelial tight junctions. Intestinal mucositis is a clinical term that is used to describe the side effects of cancer chemotherapy on the intestinal mucosa surface, resulting from dysfunction of the IMB. Typical symptoms are bloating, abdominal pain and diarrhea. Approximately 40%–100% of cancer patients undergoing chemotherapy develop mucositis[1–4], and 50% of these patients require a reduction in the dose of chemotherapy or occasional cessation of treatment. Mucositis is occasionally fatal. However, no effective treatment for mucositis has been developed.

In recent years, researchers have focused on traditional Chinese medicine for its therapeutic effects and low toxicity. *Ganoderma lucidum* (Leyss, ex Fr) Karst (G*l*) has been widely used to promote health and longevity in China for thousands of years. *Ganoderma lucidum* polysaccharides (G*l*-PS) comprise the critical biological activity components of G*l*. G*l*-PS have been reported to prevent oxidative damage[5], protect the liver, and reduce serum glucose levels without causing toxicity[6, 7]. In addition, G*l*-PS modify biological and immune responses[8].

Unfortunately, little attention has been paid to the effects of G*l*-PS on gastrointestinal mucosal function. In this study, we used a murine model of intestinal damage that was induced using methotrexate (MTX), which is a folate antagonist, to evaluate the protective role of G*l*-PS in IMB. The intestinal epithelial cell line IEC-6 was also used as an *in vitro* wounding

* To whom correspondence should be addressed.
E-mail lwdpharma@126.com
Received 2011-05-06 Accepted 2011-08-12

model to evaluate the role of G*l*-PS on epithelial cell proliferation and cell restitution to elucidate the possible action mechanisms of G*l*-PS in the treatment of IMB.

Materials and methods

Materials

Ganoderma lucidum polysaccharides (G*l*-PS) were isolated from boiling water extracts of fruit bodies of *Ganoderma lucidum* (Leyss, ex Fr) Karst followed by ethanol precipitation, dialysis and protein depletion using the Sevag method. G*l*-PS is glycopeptide with a molecular weight of 584 900. The ratio of polysaccharides to peptides is 93.61%: 6.49%. The polysaccharides consisted of *D*-rhamnose, *D*-xylose, *D*-fructose, *D*-galactose, *D*-mannose and *D*-glucose with a molar ratio of 0.793:0.964:2.944:0.167:0.389:7.94. The polysaccharides were linked together by β-glycosidic linkages. G*l*-PS is a hazel-colored water-soluble powder that was kindly provided by the Fuzhou Institute of Green Valley Bio-Pharm Technology.

Inbred female BALB/c mice (7–8 weeks old) were purchased from the Department of Experimental Animals at the Health Science Centre at Peking University in Beijing, China. The animals were housed in environmentally controlled conditions with 12-h light/12-h dark cycles and were allowed free access to water and standard laboratory chow.

IEC-6 cells were obtained from the Cell Bank of Peking Union Medical College (Beijing, China). IEC-6 cells were routinely maintained in the presence of Dulbecco's modified Eagle's medium (DMEM) (Gibco BRL, USA) containing 5% inactivated fetal calf serum (FCS), 10 μg/mL insulin, 2.8 g/L sodium bicarbonate, 100 U/mL penicillin G sodium and 100 μg/mL streptomycin sulfate.

MTX was purchased from Zhejiang Hengrui Pharmaceutical Co, Ltd. Malondialdehyde (MDA) and superoxide dismutase (SOD) analysis kits were purchased from the Nanjing Jiancheng Biology Research Center. The TGFβ ELISA kit was purchased from Wuhan Boster Bio-engineering Co, Ltd. Primary, and secondary antibodies for the measurement of IgA were obtained from Sigma Chemical Co.

Murine MTX-induced enteritis model

The animals were randomly assigned to five groups that contained nine animals each. Mice received ig once daily for 10 consecutive days of (1) low-dose G*l*-PS (50 mg/kg), (2) intermediate-dose G*l*-PS (100 mg/kg), (3) high-dose G*l*-PS (200 mg/kg), (4) vehicle (*ie*, sterile physiological saline), which was used as a model control, and (5) vehicle (*ie*, sterile physiological saline) as a normal control. With the exception of group (5), the mice were injected intraperitoneally (ip) with MTX (50 mg/kg) on the 7th d and 8th d. Two days after completing the course of MTX (the 11th d), the mice were sacrificed by cervical dislocation. Subsequently, the intestinal tissue samples were harvested and prepared for histological studies. The other segments of the intestine were removed to determine MDA and SOD levels. Before the mice were sacrificed, blood samples were obtained from each animal to perform biochemical analyses (plasma IgA level). The experiments were approved by the Animal Care and Research Ethics Committee of the Peking University Health Science Center.

Intestinal morphology and histopathology

Tissue samples of the intestine (0.5 cm) were obtained at a distance of 15 cm from the pylorus of each animal following laparotomy. Imaging using light microscopy (LM) and transmission electronic microscopy (TEM) was performed for morphological and histopathological studies. The tissue sections were stained with hematoxylin and eosin for imaging using LM.

Measurement of MDA and SOD levels

Quantitative MDA and SOD measurements were performed with tissues that were obtained from the intestine using the MDA and SOD analysis kits.

Measurement of total immunoglobulin A

A sandwich ELISA technique was used as previously described[9].

Determination of IEC-6 cell proliferation

IEC-6 cells (3×10^4) were seeded into 96-well plates (Costar, USA) in the presence of DMEM containing 5% FCS. The cultures were treated with different concentrations of G*l*-PS. After 44 h of incubation at 37 °C and 5% CO_2, a colorimetric MTT assay was performed as previously described[10]. The cultures were incubated with tetrazolium salt thiazolyl blue (20 μL) at a concentration of 5 mg/mL for another 4 h. The cell supernatants were discarded, and the cells were lysed using dimethyl sulfoxide (DMSO). The metabolization of MTT directly correlates with the cell number and was quantitated by measuring the absorbance at 570 nm (reference wavelength 450 nm) using a microplate-reader.

Determination of ODC and c-Myc mRNA expression profiles using RT-PCR analysis

The mRNA expression profiles of ODC and c-Myc in IEC-6 cells were evaluated using reverse transcription polymerase chain reaction (RT-PCR) with the Access RT-PCR system (Takara, Japan) according to the manufacturer's procedures. IEC-6 cells that were treated with or without G*l*-PS were harvested after 12 h of incubation. The total RNA was extracted using TRIzol Reagent (Invitrogen, USA). The concentration of RNA was spectrophotometrically quantified. The cDNA was synthesized using the Advantage RT-for-PCR kit protocol (Promega, USA). Diluted aliquots from these reactions were subsequently used as templates for PCR.

Commercial primers to rat glyceraldehyde 3-phosphate-dehydrogenase (GAPDH) (sense, 5′-GCCAAGGTCATCCATGACAAC-3′ and antisense, 5′-GTCCACCACCCTGTTGCTGTA-3′), rat ODC (sense, 5′-TGCTTGACATTGGTGGTG-3′ and antisense, 5′-TTCTCATCTGGCTTGGGT-3′) and rat c-Myc (sense, 5′-GCTCGCCCAAATCCTGTA-3′ and antisense, 5′-ACCCTGCCACTGTCCAAC-3′) were provided by Shanghai Sangon Biological Engineering Technology and Service Co,

Ltd (Beijing, China) were used to generate products of 498 bp, 355 bp and 385 bp, respectively. The PCR reactions included 0.4 μmol/L of each primer, 0.2 mmol/L dNTPs, 1×PCR-Buffer with 15 mmol/L $MgCl_2$ and 2 U/μL Taq polymerase (Takara, Japan). The PCR cycling protocol was as follows: 45 s at 94 °C, 45 s at 60 °C (GAPDH), 57 °C (ODC), or 59 °C (c-Myc) and 2 min at 72 °C. This protocol was performed for 24 (GAPDH)/26 (ODC)/26 (c-Myc) cycles and included an initial 5-min denaturation at 94 °C and a final 10-min extension at 72 °C. The performed cycles of PCR was chosen to ensure the exponential amplification of all specific cDNA products. The PCR-amplified samples were electrophoresed using 1.5% agarose gels, stained with ethidium bromide, visualized via UV transillumination and quantified via densitometry scanning using AlphaEaseFC V4.0.0 software (Alpha Innotech Corp). ODC and c-Myc expression profiles were normalized relative to that of GAPDH.

Monolayer wounding and measurement of epithelial cell restitution

IEC-6 cell restitution assays were performed using a modified version of a previously described technique[11, 12]. IEC-6 cells were plated in six-well polystyrene plates (Costar) with normal growth medium and allowed to reach confluence. A denuded epithelial wound was created in a standardized fashion by scraping the IEC-6 monolayers with a 200-μL pipet tip. After the scraping, the cells were washed twice with D-Hanks' buffer to remove residual cell debris. The wounded monolayers were cultured for 42 h in DMEM containing 2% FCS in the presence or absence of G*l*-PS. Wound areas were viewed under the microscope at various time points after wounding and photographed with an Olympus IX71 microscope. The denuded wound area (ROI, region of interest) was quantified using LEICA QWIN software (Germany). Two wound areas per well were analyzed. Each group was tested in triplicate, and at least three independent experiments were performed. Restitution was calculated as the migration ratio using the following equation: $(ROI_{0\ h}-ROI_{42\ h})/ROI_{0\ h}\times100\%$. The data are expressed as the mean value±SD (standard deviation) representing at least three independent experiments.

IEC-6 cell supernatant collection and determination of TGFβ levels

The collection of IEC-6 cell supernatants was performed as previously described[13]. IEC-6 cells were plated in 6-well culture dishes at a density of 2.5×10^5 cells/dish. After 24 h, the medium was replaced with medium that had been supplemented with different concentrations of G*l*-PS. IEC-6 monolayers were wounded using a 200-μL pipet tip as previously described. The cells were washed twice with D-Hanks' buffer and subsequently incubated with fresh medium that had been supplemented with G*l*-PS. After 24 h, the cell supernatants were collected. Secretion of TGFβ from supernatants was determined using a sandwich ELISA kit according to the manufacturer's protocol.

Statistical analysis

The data were analyzed using one-way ANOVA followed by the least-significant difference (LSD) test. *P* values that were below 0.05 were considered statistically significant.

Results

Morphological and histological results

As shown in Figure 1, G*l*-PS did not perturb the morphological and histological features of the jejunum in mice. All tissue sections of the intestine of the control group were normal. In the tissue sections of the MTX-treated mice, we observed villus shortening, variable degrees of fusion, epithelial atrophy, a decreased number of crypt cells, crypt loss and the development of abscesses in crypts. In addition, we noted an inflammatory infiltration in the lamina propria. The number of goblet cells was significantly decreased in the villi and the crypts. Although the histopathological features in the MTX+G*l*-PS 100 mg/kg-treated group were similar to the findings in the MTX-treated group, the total small intestine damage in the MTX+G*l*-PS 100 mg/kg-treated group was less than that of the MTX-treated group.

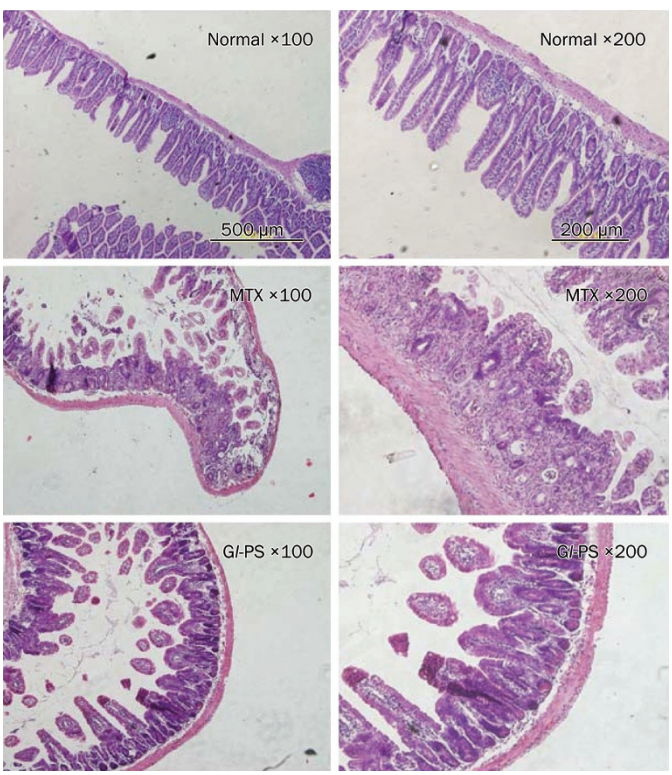

Figure 1. Morphology of the murine jejunum under magnification of 100 and 200. Normal: group of normal control; MTX: group of MTX model; G*l*-PS: group of 100 mg/kg G*l*-PS under MTX stress. These photographs are representative examples of a group of nine mice.

Examination of the intestinal ultrastructure revealed that the microvilli in the normal control group were long, abun-

dant and neatly arranged, whereas the microvilli in the MTX-treated group were reduced, shortened and disordered. Some of the microvilli were ablated. Swelling of the nuclear membrane and mitochondria was observed. The intestinal ultrastructural changes in the MTX+G*l*-PS 100 mg/kg-treated group were ameliorated compared to those in the MTX-treated group (Figure 2).

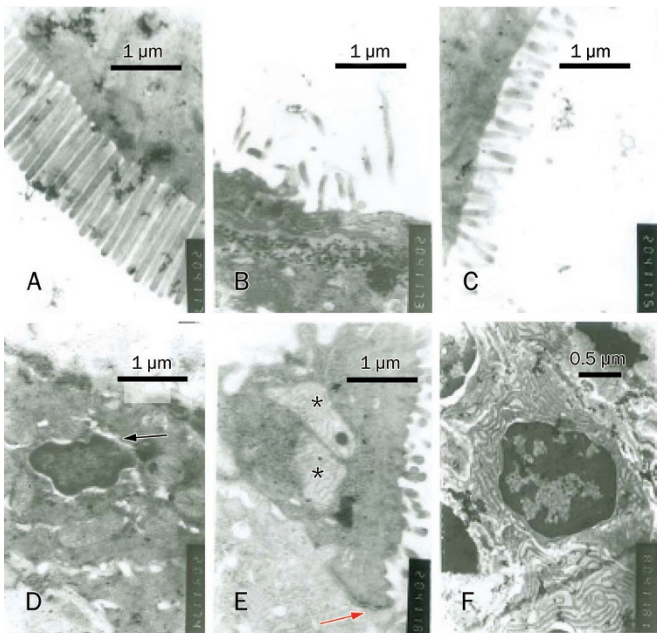

Figure 2. Changes of intestinal ultrastructure. (A) normal control group. (B, D, E) MTX model group. (C, F) group of 100 mg/kg G*l*-PS under MTX stress. The arrow (D) indicates swelling of nuclear membrane. The arrow (D, E) indicates tight junction. * indicates swelling of mitochondria.

G*l*-PS decreased MDA levels but increased SOD levels in mice intestine

We showed that the concentration of MDA in the intestine of mice in the MTX-treated group was significantly higher than that in the normal control group (P<0.001). However, we observed decreases in MDA concentration in MTX+G*l*-PS groups in a dose-dependent manner (Figure 3). However, the level of SOD in the MTX model group was down-regulated compared to that in the control group (P<0.01). MTX-induced decreases in SOD responded to G*l*-PS treatment in a dose-dependent manner (P<0.05) (Figure 4).

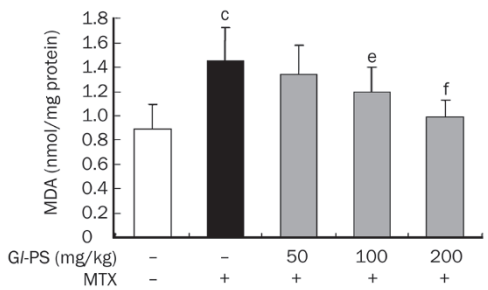

Figure 3. Effect of G*l*-PS on MDA content in supernatant homogenate for intestine in MTX-induced mice. n=9. Mean±SD. ^{c}P<0.01 *vs* normal control. ^{e}P<0.05, ^{f}P<0.01 *vs* MTX model.

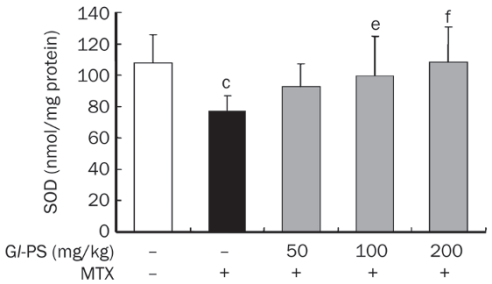

Figure 4. Effect of G*l*-PS on SOD content in supernatant homogenate of intestine in MTX induced mice. n=9. Mean±SD. ^{c}P<0.01 *vs* normal control. ^{e}P<0.05, ^{f}P<0.01 *vs* MTX model.

The concentration of IgA in serum

The concentration of total serum IgA was measured using an ELISA. MTX treatment significantly decreased the total serum IgA concentration compared to the normal control (P<0.05). G*l*-PS treatment elevated the concentration of IgA in a dose-dependent manner (Figure 5).

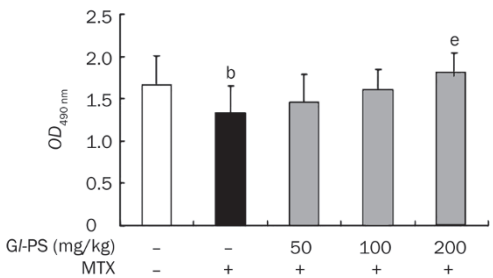

Figure 5. Effect of G*l*-PS on serum IgA level in MTX-induced mice. IgA level show by OD_{490} value. n=7. Mean±SD. ^{b}P<0.05 *vs* normal. ^{e}P<0.05 *vs* MTX model.

Effect of G*l*-PS on the proliferation of IEC-6 cells

The cells were incubated with different concentrations of G*l*-PS (0.1, 1, and 10 μg/mL) for 48 h. As shown in Table 1,

Table 1. Effects of G*l*-PS on IEC-6 cells proliferation. n=8. Mean±SD. ^{b}P<0.05, ^{c}P<0.01 *vs* DMEM.

Group	*OD* value (570 nm)
DMEM	0.626±0.072
G*l*-PS 0.1 μg/mL	0.725±0.080^{b}
G*l*-PS 1 μg/mL	0.751±0.075^{c}
G*l*-PS 10 μg/mL	0.840±0.077^{c}

G*l*-PS significantly promoted the proliferation of IEC-6 cells in a dose-dependent manner compared to the control. The proliferation rate was 34% higher in cells that were treated with 10 μg/mL G*l*-PS compared to that in control cells.

G*l*-PS modulated mRNA expression profiles of ODC and c-Myc in IEC-6 cells

Semiquantitative RT-PCR was used to determine the effect of G*l*-PS on ODC and c-Myc mRNA expression profiles in IEC-6 cells. As shown in Figures 6 and 7, ODC and c-Myc mRNAs were expressed in IEC-6 cells. G*l*-PS (10 and 20 μg/mL) treatment significantly up-regulated the expression of ODC and c-Myc mRNAs compared with that in the normal control group (Figures 6 and 7).

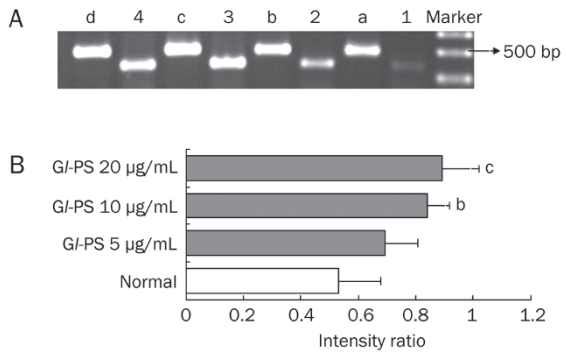

Figure 6. The mRNA expression of ODC and GAPDH in IEC-6 cells by RT-PCR. (A) 1–4: IEC-6 cells were treated with 0, 5, 10, and 20 μg/mL G*l*-PS and it is mRNA expression of ODC. a–d: IEC-6 cells were treated with 0, 5, 10, and 20 μg/mL G*l*-PS and it is mRNA expression of GAPDH. (B) PCR products were quantified by densitometric scanning and ODC expression was normalized relative to the steady-state expression of GAPDH used as internal control (intensity ratio: ODC to GAPDH). Values represent means±SD from three independent experiments. $^{b}P<0.05$, $^{c}P<0.01$ *vs* normal.

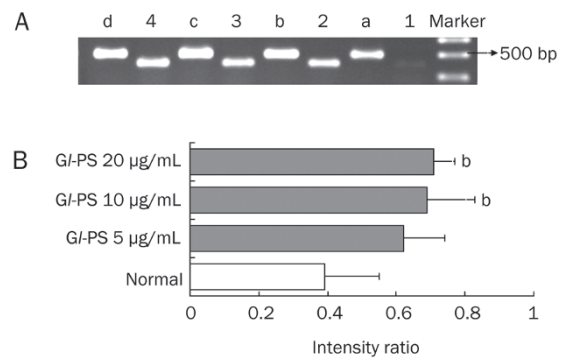

Figure 7. The mRNA expression of c-Myc and GAPDH in IEC-6 cells by RT-PCR. (A) 1–4: IEC-6 cells were treated with 0, 5, 10, and 20 μg/mL G*l*-PS and it is mRNA expression of c-Myc. a–d: IEC-6 cells were treated with 0, 5, 10, and 20 μg/mL G*l*-PS and it is mRNA expression of GAPDH. (B) Quantification of RT-PCR data. $n=3$. $^{b}P<0.05$ *vs* normal control.

G*l*-PS enhanced IEC-6 cell restitution

As shown in Table 2, G*l*-PS caused a dose-dependent enhancement of intestinal epithelial cell restitution in a well-established wounding model with IEC-6 cell monolayers. We detected a 36% increase in the restitution of IEC-6 cells that were treated with 10 μg/mL G*l*-PS compared to that of control cells.

Table 2. The effect of G*l*-PS on IEC-6 cells wound restitution. $n=8$. Mean±SD. $^{b}P<0.05$, $^{c}P<0.01$ *vs* DMEM.

Group	*OD* value (570 nm)
DMEM	0.486±0.054
G*l*-PS 0.1 μg/mL	0.544±0.062
G*l*-PS 1 μg/mL	0.587±0.046[b]
G*l*-PS 10 μg/mL	0.661±0.089[c]

Effects of G*l*-PS on TGFβ levels in IEC-6 cell culture supernatants

Recent evidence has supported a central role for TGFβ in the process of intestinal epithelial restitution[14]. Therefore, the production of TGFβ was measured to determine the possible involvement of this cytokine in G*l*-PS-mediated restitution. No significant effect was observed on the production of TGFβ following G*l*-PS treatment (Table 3).

Table 3. Effects of G*l*-PS on TGFβ level in IEC-6 cells culture supernatants. Values represent means (±SD) from three independent experiments performed in duplicate.

Group	TGFβ (pg/mL)
DMEM	9.602±0.001
G*l*-PS 5 μg/mL	9.603±0.001
G*l*-PS 10 μg/mL	9.605±0.001
G*l*-PS 20 μg/mL	9.607±0.002

Discussion

The intestinal epithelial barrier, including the biotic, mechanical and immunity barriers, is a crucial barrier against pathogen infection. Previous studies have not demonstrated an effective method to prevent IMB damage[15]. It is necessary to develop natural medicines that are effective in treating IMB dysfunction and intercurrent diseases. In the current report, the effects of G*l*-PS on the intestinal epithelial barrier were investigated.

Chemotherapy commonly produces structural damage to the intestinal mucosa in cancer patients[16] and causes side effects such as severe enterocolitis. In agreement with previous studies[17], the results of the present study reveal that MTX induced small intestinal injury, which is characterized by villus shortening and fusion, epithelial atrophy, crypt loss,

inflammatory infiltration of the lamina propria, and goblet cell depletion. G*l*-PS treatment reduced intestinal mucosal damage in this study and reduced gastric mucosal lesions in a previous study[18].

Increased oxidative stress and decreased antioxidant defenses have been demonstrated in intestinal mucosal biopsies of patients with MTX-induced damage to the small intestinal epithelium. These damages may be reduced by antioxidant agents. As previously reported, protective effects of various antioxidants, such as curcumin[19], aged garlic extract[20] and N-acetylcysteine[17], have been shown in MTX-induced small intestinal damage. MDA is frequently used in the measurement of lipid peroxide levels and correlates with the degree of lipid peroxidation. SOD levels correlate with the elimination of free radicals. G*l*-PS have been widely used as antioxidants *in vivo* and *in vitro*[21–23]. Therefore, in the present study, we investigated whether G*l*-PS inhibit MTX-induced small intestine damage via decreasing MDA levels and increasing SOD levels. We showed that the MDA level in the small intestinal mucosa of MTX-treated mice was remarkably increased, suggesting that MTX treatment caused oxidative damage and lipid peroxidation in the intestinal mucosa. MTX-induced increases in MDA levels were attenuated after G*l*-PS administration (Figure 3). These findings may indicate that G*l*-PS protect intestinal tissue against MTX-induced lipid peroxidation. The present study also demonstrated that the MTX-induced downregulation of SOD was inhibited by G*l*-PS treatment in the intestinal mucosa of mice (Figure 4). These results suggest that the effects of G*l*-PS may be achieved via its antioxidant and free radical-eliminating activities.

Immunoglobulin A (IgA) is an important component of the intestinal immunological barrier and is the most abundant immunoglobulin at the mucosal surface where it plays crucial role in mucosal protection[24]. The protective barrier of the gastrointestinal system is impaired in IgA deficiency, and IgA-deficient individuals tend to develop gastrointestinal infections[25, 26]. G*l*-PS are well-known modulators of the immune system[27, 28]. In this study, we found that MTX-treated mice displayed a reduced level of serum IgA. This result indicates that mucosal immune barrier dysfunction occurs during MTX-induced intestine damage. G*l*-PS restored the level of IgA, suggesting that G*l*-PS bolstered intestinal immunity.

Observations over the past several years have demonstrated the ability of the gastrointestinal tract to rapidly restore the continuity of the surface epithelium after extensive destruction. Three different phases have been identified. First, epithelial cells that are adjacent or just beneath the injured surface migrate into the wound to cover the denuded area, which is a process that has been termed epithelial restitution. Secondly, epithelial cell proliferation takes place to replenish the decreased cell pool. Finally, maturation and differentiation of epithelial cells enable the epithelium to maintain its functional activities[12]. The initial mechanism contributing to rapid resealing of epithelial defects after mucosal injury is the migration of viable epithelial cells from the wound margin into the denuded area, which is a process that does not require cell proliferation[29]. The data presented in this study revealed that G*l*-PS at a concentration of 10 μg/mL augmented the migration of intestinal epithelial cells in an *in vitro* model that mimicked the early cell division-independent stages of epithelial restitution. When G*l*-PS were added immediately after wounding, they significantly increased intestinal epithelial cell migration in a dose-dependent manner. Although the exact mechanism of restitution has not been elucidated, the cytokine TGFβ has been shown to play an important role in the stimulation of cell migration after wounding. Some studies have revealed that the intestinal epithelial cell restitution process is stimulated via a TGFβ-dependent pathway[30, 31]. However, in other cases, the intestinal epithelial cell restitution was independent of TGFβ[32]. In our study, we found that G*l*-PS did not affect TGFβ expression in IEC-6 cells after wounding. These results may indicate that G*l*-PS stimulate restitution possibly through a TGFβ-independent pathway.

Epithelial cell proliferation, which is another essential mechanism to mediate resealing of mucosal wounds in the intestine, was substantially promoted by G*l*-PS treatment in our investigation. This effect was dose-dependent, and maximal effects were detected at a concentration of 10 μg/mL G*l*-PS.

The polyamines are a group of ubiquitously distributed organic cations that are intimately involved in the regulation of gastrointestinal mucosal growth[33]. ODC, which is a pyridoxal phosphate-dependent enzyme, is the first rate-limiting enzyme for the biosynthesis of polyamines. The extent of the ODC mRNA expression correlates with the cell proliferation. Treatment of gastrointestinal origin cells with difluoromethylornithine, which is a suicide substrate inhibitor of ODC and induces depletion of intracellular polyamines, inhibits proliferation[34, 35]. In addition, induction of the ODC gene may play an important role in the signaling pathways that are associated with several oncogenes. Transformation by activated *ras*, *v-src* and *myc* appears to be tightly coupled to ODC gene expression and polyamine accumulation[36–38]. ODC is a transcriptional target of c-Myc[39], which has a central role in the proliferation of normal cells. Following mitogenic stimulation of quiescent cells, c-Myc is rapidly induced and remains elevated, suggesting that it is required for continuous cell growth[40]. In the present study, an increase in *c-Myc* and *ODC* gene expression (Figure 6 and 7) was observed in IEC-6 cells 12 h after exposure to G*l*-PS. *c-Myc* and *ODC* gene expression were coincident to the stimulatory effect on cell proliferation (Table 1).

In summary, the present study demonstrated that G*l*-PS reduced MTX-induced intestinal toxicity. We demonstrated that G*l*-PS increased the antioxidation and intestinal immunity *in vivo*, accelerated wound repair by stimulating cell proliferation and migration *in vitro*, and up-regulated *c-Myc* and *ODC* mRNA expression. However, G*l*-PS had no effects on TGFβ levels. Altogether, we demonstrated a new protective effect of G*l*-PS on the intestinal barrier via induction of epithelial cell proliferation and migration. The present study may provide a pharmacological basis for the clinical use of G*l*-PS in preventing enteritis in patients receiving chemotherapeutic agents. Previous studies have shown that cell differentiation

also plays an important role in protecting the intestinal barrier. However, the effect of *Gl*-PS on cell differentiation was not assessed in this study. Therefore, further investigation is required using molecular markers such as sucrase-isomaltase and alkaline phosphatase.

Acknowledgements

The authors are grateful to Dr Mei-hua BAO for her critical reading of the manuscript.

Author contribution

Li-hua CHEN, Wei-dong LI, and Z hi-bin LIN designed the research; Li-hua CHEN performed the research; Wei-dong LI and Zhi-bin LIN contributed new analytical reagents and tools; Li-hua CHEN and Wei-dong LI analyzed the data; and Li-hua CHEN wrote the paper.

References

1 Gupta G, Agarwala S, Thulkar S, Shukla B, Bakhshi S. Jejunal stricture: a rare complication of chemotherapy in pediatric gastrointestinal B-cell non-Hodgkin lymphoma. J Pediatr Hematol Oncol 2011; 33: e69–71.

2 Nicoletto MO, Dalla Palma M, Donach ME, Gusella M, Cappetta A, Shams M, *et al*. Positive experience of intraperitoneal chemotherapy followed by intravenous chemotherapy in heavily pretreated patients with suboptimal residual ovarian cancer and primary peritoneal cancer. Tumori 2010; 96: 918–25.

3 Prisciandaro LD, Geier MS, Butler RN, Cummins AG, Howarth GS. Evidence supporting the use of probiotics for the prevention and treatment of chemotherapy-induced intestinal mucositis. Crit Rev Food Sci Nutr 2011; 51: 239–47.

4 Van Vliet MJ, Harmsen HJ, de Bont ES, Tissing WJ. The role of intestinal microbiota in the development and severity of chemotherapy-induced mucositis. PLoS Pathog 2010; 6: e1000878.

5 You YH, Lin ZB. Protective effects of *Ganoderma lucidum* polysaccharides peptide on injury of macrophages induced by reactive oxygen species. Acta Pharmaco Sin 2002; 23: 787–91.

6 Zhang GL, Wang YH, Ni W, Teng HL, Lin ZB. Hepatoprotective role of *Ganoderma lucidum* polysaccharide against BCG-induced immune liver injury in mice. World J Gastroenterol 2002; 8: 728–33.

7 Zhang HN, He JH, Yuan L, Lin ZB. *In vitro* and *in vivo* protective effect of G*anoderma lucidum* polysaccharides on alloxan-induced pancreatic islets damage. Life Sci 2003; 73: 2307–19.

8 Zhu XL, Lin ZB. Modulation of cytokines production, granzyme B and perforin in murine CIK cells by *Ganoderma lucidum* polysaccharides. Carbohydrate Polymers 2006; 63: 188–97.

9 Ha CL. The inhibitory effect of the Chinese herb *Ganoderma lucidum* mycelium on gut immunoglobulin A responses to cholera toxin in mice. Nutr Res 2003; 23: 691–701.

10 Mossman T. Rapid colorimetric assay for cellular growth and survival: application to proliferation and cytotoxity assays. J Immunol Methods 1983; 65: 55–63.

11 Zou L, Sato N, Kone BC. α- Melanocyte stimulating hormone protects against H_2O_2-induced inhibition of wound restitution in IEC-6 cells via a Syk kinase and NF-κB dependent mechanism. Shock 2004; 22: 453–9.

12 Jung S, Fehr S, Harder-d'Heureuse J, Wiedenmann B, Dignass AU. Corticosteroids impair intestinal epithelial wound repair mechanisms *in vitro*. Scand J Gastroenterol 2001; 36: 963–70.

13 Ruthig DJ, Meckling-Gill KA. N-3 and n-6 fatty acids stimulate restitution by independent mechanisms in the IEC-6 model of intestinal wound healing. J Nutr Biochem 2002; 13: 27–35.

14 Dignass AU, Podolsky DK. Cytokine modulation of intestinal epithelial cell restitution: central role of transforming growth factorβ. Gastroenterology 1993; 105: 1323–32.

15 Daniel C, Baumgart, Dignass AU. Intestinal barrier function. Curr Opin Clin Nutr Metab Care 2002; 5: 685–94.

16 Cunningham D, Morgan RJ, Mills PR, Nelson LM, Toner PG, Soukop M, *et al*. Functional and structural changes of the human proximal small intestine after cytotoxic therapy. J Clin Pathol 1985; 38: 265–70.

17 Ciralik H, Bulbuloglu E, Cetinkaya A, Kurutas EB, Celik M, Polat A. Effects of N-acetylcysteine on methotrexate-induced small intestinal damage in rats. Mt Sinai J Med 2006; 73: 1086–92.

18 Gao Y, Zhou S, Wen J, Huang M, Xu A. Mechanism of the antiulcerogenic effect of *Ganoderma lucidum* polysaccharides on indomethacin-induced lesions in the rat. Life Sci 2002; 72: 731–45.

19 Song WB, Wang YY, Meng FS, Zhang QH, Zeng JY, Xiao LP, *et al*. Curcumin protects intestinal mucosal barrier function of rat enteritis via activation of MKP-1 and attenuation of p38 and NF-κB activation. PLoS One 2010; 5: 1–11.

20 Yüncü M, Eralp A, Celik A. Effect of aged garlic extract against methotrexate-induced damage to the small intestine in rats. Phytother Res 2006; 20: 504–10.

21 Sudheesh NP, Ajith TA, Ramnath V, Janardhanan KK. Therapeutic potential of *Ganoderma lucidum* (Fr) P Karst against the declined antioxidant status in the mitochondria of post-mitotic tissues of aged mice. Clin Nutr 2010; 29: 406–12.

22 Liu W, Wang H, Pang X, Yao W, Gao X. Characterization and antioxidant activity of two low-molecular-weight polysaccharides purified from the fruiting bodies of *Ganoderma lucidum*. Int J Biol Macromol 2010; 46: 451–7.

23 Cherian E, Sudheesh NP, Janardhanan KK, Patani G. Free-radical scavenging and mitochondrial antioxidant activities of Reishi-Ganoderma lucidum (Curt: Fr) P Karst and Arogyapacha-Trichopus zeylanicus Gaertn extracts. J Basic Clin Physiol Pharmacol 2009; 20: 289–307.

24 Kadaoui KA, Corthésy B. Secretory IgA mediates bacterial translocation to dendritic cells in mouse Peyer's patches with restriction to mucosal compartment. J Immunol 2007; 179: 7751–7.

25 Yel L. Selective IgA deficiency. J Clin Immunol 2010; 30: 10–6.

26 Brandtzaeq P. Update on mucosal immunoglobulin A in gastrointestinal disease. Curr Opin Gastroenterol 2010; 26: 554–63.

27 Zhang J, Tang Q, Zhou C, Jia W, Da Silva L, Nguyen LD, *et al*. GLIS, a bioactive proteoglycan fraction from *Ganoderma lucidum*, displays anti-tumour activity by increasing both humoral and cellular immune response. Life Sci 2010; 87: 628–37.

28 Huang SQ, Li JW, Wang Z, Pan HX, Chen JX, Ning ZX. Optimization of alkaline extraction of polysaccharides from *Ganoderma lucidum* and their effect on immune function in mice. Molecules 2010; 15: 3694–708.

29 Rutten MJ, Ito S. Morphology and electrophysiology of guinea pig gastric mucosal repair *in vitro*. Am J Physiol 1983; 244: G171–82.

30 Strauch ED, Wang JY, Bass BL. Bile salt stimulates intestinal epithelial cell migration through TGFbeta after wounding. J Surg Res 2001; 97: 49–53.

31 Bulut K, Meier JJ, Ansorge N, Felderbauer P, Schmitz F, Hoffmann P, *et al*. Glucagon-like peptide 2 improves intestinal wound healing through induction of epithelial cell migration *in vitro*-evidence for a TGF-β-mediated effect. Regul Pept 2004; 121: 137–43.

32 Paclik D, Lohse K, Wiedenmann B, Dignass AU, Sturm A. Galectin-2

and -4, but not galectin-1, promote intestinal epithelial wound healing *in vitro* through a TGF-beta-independent mechanism. Inflamm Bowel Dis 2008; 14: 1366–72.

33 Seidel ER, Scemama JL. Gastrointestinal polyamines and regulation of mucosal growth. Nutrit Biochem 1997; 8: 104–11.

34 Ye YN, Liu ES, Shin VY, Koo MW, Li Y, Wei EQ, *et al.* A mechanistic study of proliferation induced by *Angelica sinensis* in a normal gastric epithelial cell line. Biochem Pharmacol 2001; 61: 1439–48.

35 Lefevre PL, Palin MF, Chen G, Turecki G, Murphy BD. Polyamines are implicated in the emergence of the embryo from obligate diapause. Endocrinology 2011; 152: 1627–39.

36 Hölttä E, Sistonen L, Alitalo K. The mechanism of ornithine decarboxylase deregulation in c-Ha-*ras* oncogene-transformed NIH 3T3 cells. J Biol Chem 1988; 263: 4500–7.

37 Guerrero I, Pellicer A, Alitalo K. Dissociation of *c-fos* from ODC expression and neuronal differentiation in a PC12 subline stably transfected with an inducible n-*ras* oncogene. Biochem Biophys Res Commun 1988; 150: 1185–92.

38 Celano P, Baylin SB, Giardello FM, Nelkin BD, Casero RA. Effect of polyamine depletion on c-myc expression in human colon carcinoma cells. J Biol Chem 1988; 263: 5491–4.

39 Bello-Fernandez C, Packham G, Cleveland JL. The ornithine decarboxylase gene is a transcriptional target for c-Myc. Proc Natl Acad Sci U S A 1993; 90: 7804–8.

40 Evan G, Littlewood TD. The role of c-myc in cell growth. Curr Opin Genet Dev 1993; 3: 44–9.